A Forward Converter Without Commutation Losses Due To The Use Of One Non-Dissipative Snubber

Barreto, L. H. S. C.; Pereira, A. A. (**); Farias, V. J.; Freitas, L. C. de and Vieira Jr., J. B.

Universidade Federal de Uberlândia
Centro de Ciências Exatas e Tecnologia
Departamento de Engenharia Elétrica
Campus Santa Mônica - Bloco "3N"
38400-902 - Uberlândia - MG – Brazil
Phone: 55 34 239-4166 FAX: 55 34 239-4166
Email: batista@ufu.br

(**) Universidade Federal de Goiás
Departamento de Computação
Campus Avançado de Catalão
CEP: 75.704-020 - Catalão - GO - Brazil
FAX: 55 62-441-3488

Abstract - This paper presents a Forward converter with a non-dissipative snubber, which provides a soft switching converter operation. This approach allows the main switch to work in a ZVS way and the auxiliary switch to work in a ZCS way. Two capacitors (resonant capacitors), one inductor (resonant inductor), one switch (auxiliary switch) and one diode in series with the main switch compose the non-dissipative snubber. The complete operating principle, relevant equations and simulation and experimental results are presented.

1 - INTRODUCTION

In the last years, size, weight, cost and EMI reduction in the Switching Mode Power Supplies (SMPS) has been the workhorse of the industry and academic researches. One way to achieve some of these features in SMPS is increasing switching frequency. To obtain high switching frequency is necessary attaining high efficiency in converter operation.

Those operational features can not be normally achieved in the hard switching power converter technology. So, in this way, lossless commutation converters approach must be used. During the last few years many soft switching converters have been developed. As example, Zero Current Switching (ZCS) and Zero Voltage Switching (ZVS) were reported in the reference [1].

However, these converters present severe load limitation due to the current and/or voltage peak on the switches as well as variable switching frequency which imposes large output filters design to attend the lowest switching frequency operation as well as the control circuit must attend the higher operation frequency. The problem of variable frequency was solved by the Quasi-Resonant PWM Converters reported in the references [2], [3], [4], [5], [6] and [7].

In order to overcome these limitations many other converters operating with fixed frequency (Pulse Width Modulated - PWM) and with lossless commutation have been presented all over the world, in a great number of publications. Among these publications we emphasize those number [8], [9], [10], [11], [12], [13] and [14].

To contribute with the general research effort this paper proposes a non-dissipative snubber associated with a Forward Converter shown in Figure 1.

2 - THE PROPOSED NON-DISSIPATIVE SNUBBER ASSOCIATED WITH A FORWARD CONVERTER

Figure 1 shows the simplified schematic circuit of the proposed non-dissipative snubber associated with a Forward Converter (FORWARD-PWM-ZVS-SR). This converter operates without commutation losses.

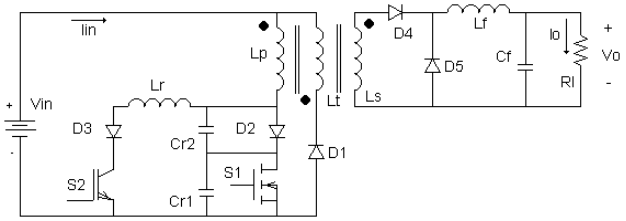

Figure 1 - Forward Converter associated with the proposed non-dissipative snubber (FORWARD-PWM-ZVS-SR).

Switches S1 and S2 have soft-commutation. Switch S1 commutates in a ZVS way and switch S2 commutates in a ZCS way.

3 - PRINCIPLE OF OPERATION

Following, a complete theoretical analysis for the approach showed in Figure 1 is presented.

The analysis begins with the description of the eleven operational stages, whose is divided a proposed converter switching cycle.

First Stage (t_0, t_1) - This stage begins when switch S2 is turned on in a ZCS way. During this stage the resonant inductor current (ILr) rises linearly from zero to the input current (Iin).

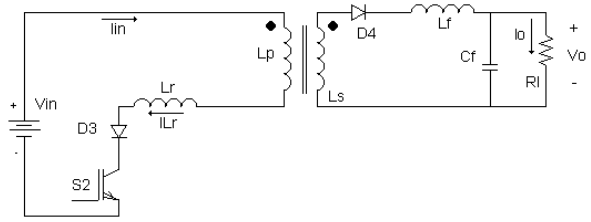

Figure 2 - First Stage (t_0, t_1).

Second Stage (t_1, t_2) - When the resonant inductor current (ILr) is equal to the input current (Iin), this stage begins. During this stage the resonance between the resonant capacitors (Cr1 and Cr2) and the resonant inductor (Lr), begins. In this stage the resonant capacitor 1 (Cr1) is discharged and the resonant capacitor 2 (Cr2) is charged. This stage finishes when the resonant capacitor 1 (Cr1) is completely discharged.

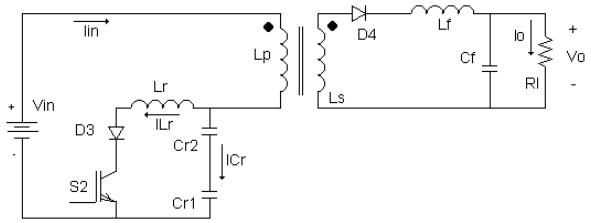

Figure 3 - Second Stage (t_1, t_2).

Third Stage (t_2, t_3) -This stage begins when the voltage on the resonant capacitor 1 (Cr1) is equal to zero. During this stage the resonant capacitor 2 (Cr2) is in resonance with the resonant inductor (Lr), alone. When the resonant inductor current is equal to zero this stage finishes. After the resonant inductor current reaches zero the switch S2 can be turned off in a ZCS way. During this stage the main switch S1 is turned on in a ZVS way.

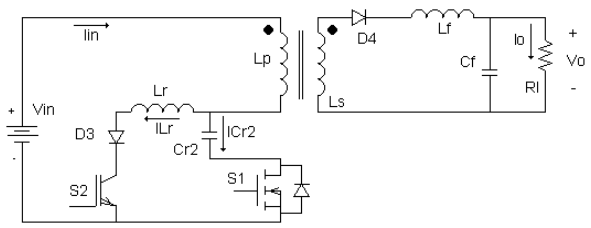

Figure 4 - Third Stage (t_2, t_3).

Fourth Stage (t_3, t_4) - This stage begins when ILr is equal to zero, and it finishes when the voltage on resonant capacitor 2 (Cr2) is zero. During this stage the resonant capacitor 2 (Cr2) is discharged in a linear way by the input current (Iin).

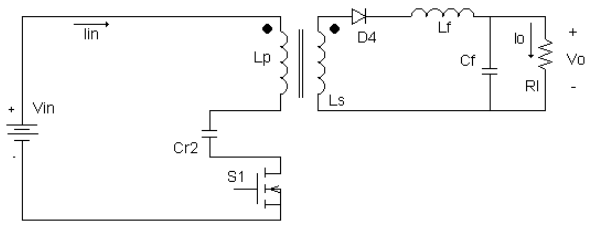

Figure 5 - Forth Stage (t_3, t_4).

Fifth Stage (t_4, t_5) - This stage begins when the voltage on the resonant capacitor 2 (Cr2) is equal to zero, turning on diode D2. When switch S1 is turned off in a ZVS way this stage finishes. During this stage the energy is transferred from the input voltage source (Vin) to the load. This stage is responsible for the converter PWM characteristics.

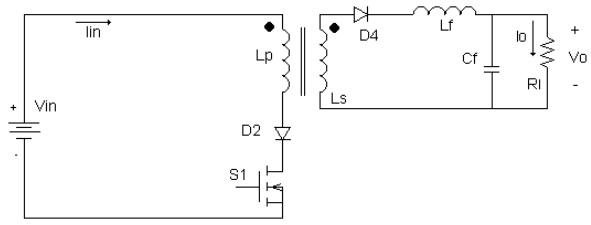

Figure 6 - Fifth Stage (t_4, t_5).

Sixth Stage (t_5, t_6) - When the main switch S1 is turned off, this stage begins. Input current flows through the resonant capacitor 1 (Cr1), this capacitor is charged up to the output voltage (Vo). This stage finishes when diode D1 is turned on beginning the transformer demagnetization.

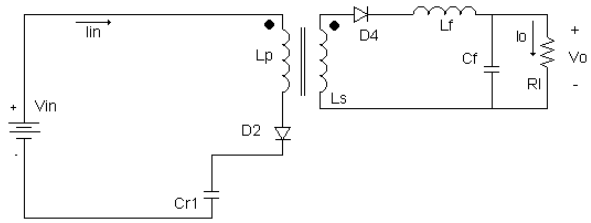

Figure 7 - Sixth Stage (t_5, t_6).

Seventh Stage (t_6, t_7) – This is the stage of the transformer demagnetization. When diode D1 is turned on, this stage begins. This stage finishes when the transformer demagnetization finishes. During this stage the transformer demagnetizes through diode D1 and Vin

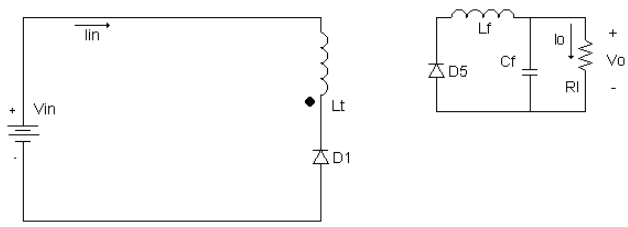

Figure 8 - Seventh Stage (t_6, t_7).

Eighth Stage (t_7, t_8) – When the transformer demagnetization finishes this stage begins. This is the freewheeling stage. During this stage the load current flows through freewheeling diode D5.

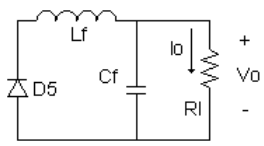

Figure 9 – Eighth Stage (t_7, t_8).

From the operating stages, described above, one can obtain the waveforms shown in Figure 10.

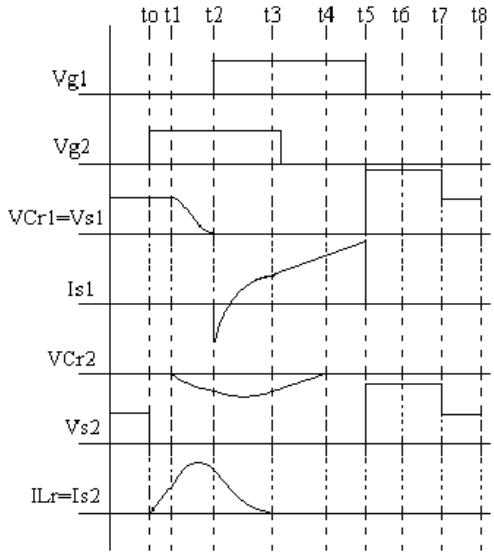

Figure 10 - Theoretical waveforms for the FORWARD-PWM-ZVS-SR.

From the equivalent circuits presented before one can obtain the FORWARD-PWM-ZVS-SR conversion ratio. This study is doing with the following assumptions:

All components and switches are ideal;
The input voltage source is ideal;
The load is an ideal current source.

First Stage (t_o, t_1)

The following equations describe this operational stage.

np = number of windings of the primary;
ns = number of windings of the secondary;
nt = number of windings of the tertiary;
fs = switching frequency ;
fo = resonant frequency;
Iin = input current;
Vin = input voltage.

$$\omega o = 2\pi fo \quad (1)$$

$$\omega s = 2\pi fs \quad (2)$$

$$\frac{1}{Cr} = \frac{1}{Cr1} + \frac{1}{Cr2} \quad (3)$$

$$Cr2 = X*Cr1 \quad (4)$$

$$\omega o = \frac{1}{\sqrt{LrCr}} \quad (5)$$

$$Zo = \sqrt{\frac{Lr}{Cr}} \quad (6)$$

$$\alpha = \frac{Iin}{Vin}\sqrt{\frac{Lr}{Cr}} \quad (7)$$

$$\alpha_2 = \frac{Iin}{Vin}\sqrt{\frac{Lr}{Cr2}} \quad (8)$$

$$Ts = \frac{1}{fs} \quad (9)$$

$$K = \left(-\alpha\sqrt{\frac{X-1}{X+1}} + \sqrt{\frac{1}{X} - \frac{\alpha^2}{X+1}}\right) \quad (10)$$

$$K1 = \frac{fs}{fo} \quad (11)$$

$$iLr(t) = \frac{Vin}{Lr}t \quad (12)$$

$$\Delta t1 = \frac{\alpha}{\omega o} \quad (13)$$

Where, the initial conditions are:

$$iLr(0) = 0 \quad (14)$$

$$vCr1(0) = Vin \quad (15)$$

$$vCr2(0) = 0 \quad (16)$$

Then,

$$iLr(\Delta t1) = Iin \quad (17)$$

$$vCr1(\Delta t1) = Vin \quad (18)$$

$$vCr2(\Delta t1) = 0 \quad (19)$$

Second Stage (t_1, t_2)

The following equations describe this operational stage.

$$iLr(t) = Iin + \frac{Vin}{Zo}\text{sen}\,\omega ot \quad (20)$$

$$vCr(t) = Vin\cos\omega ot \quad (21)$$

$$\Delta t2 = \frac{1}{\omega o}\text{Arc}\cos\left(-\frac{1}{X}\right) \quad (22)$$

Where, the initial conditions are:

$$iLr(0) = Iin \quad (23)$$

$$vCr1(0) = Vin \quad (24)$$

$$vCr2(0) = 0 \quad (25)$$

$$vCr(0) = Vin \quad (26)$$

Then,

$$iLr(\Delta t2) = Iin + \frac{Vin}{Zo}\sqrt{\frac{X^2-1}{X^2}} \quad (27)$$

$$vCr1(\Delta t2) = 0 \quad (28)$$

$$vCr2(\Delta t2) = -\frac{Vin}{X} \quad (29)$$

Third Stage (t_2, t_3)

The following equations describe this operational stage.

$$iLr(t) = Iin + \frac{Vin\sqrt{X+1}}{ZoX}\left(\sqrt{X-1}\cos\frac{\omega o}{\sqrt{X+1}}t - \text{sen}\frac{\omega o}{\sqrt{X+1}}t\right) \quad (30)$$

$$vCr2(t) = \frac{Vin}{X}\left(\sqrt{X-1}\,\text{sen}\frac{\omega o}{\sqrt{X+1}}t + \cos\frac{\omega o}{\sqrt{X+1}}t\right) \quad (31)$$

$$\Delta t3 = \frac{\sqrt{X+1}}{\omega o}\text{Arc}\cos(K) \quad (32)$$

Where, the initial conditions are:

$$iLr(0) = Iin + \frac{Vin}{Zo}\sqrt{\frac{X^2-1}{X^2}} \quad (33)$$

$$vCr2(0) = -\frac{Vin}{X} \quad (34)$$

Then,

$$iLr(\Delta t3) = 0 \quad (35)$$

$$vCr2(\Delta t3) = -\frac{Vin}{X}\left(\sqrt{(X-1)(1-K^2)} + K\right) \quad (36)$$

Fourth Stage (t_3, t_4)

The following equations describe this operational stage.

$$vCr2(t) = \frac{Iin}{Cr2}t \quad (37)$$

$$\Delta t4 = \frac{(X+1)}{X\alpha\omega o}\left(\sqrt{(X-1)(1-K^2)}+K\right) \quad (38)$$

Where, the initial conditions are:

$$iLr(0) = 0 \quad (39)$$

$$vCr2(0) = -\frac{Vin}{X}\left(\sqrt{(X-1)(1-K^2)}+K\right) \quad (40)$$

Then,

$$vCr2(\Delta t4) = 0 \quad (41)$$

Fifth Stage (t_4, t_5)

The following equation describe this operational stage.

$$\Delta t5 = D.Ts - \Delta t4 - \Delta t3 \quad (42)$$

Sixth Stage (t_5, t_6)

The following equations describe this operational stage.

$$vCr1(t) = \frac{Iin}{Cr1}t \quad (43)$$

$$\Delta t6 = \frac{(X+1)}{X\alpha\omega o}\left(1+\frac{np}{nt}\right) \quad (44)$$

Where, the initial conditions are:

$$vCr1(0) = 0 \quad (45)$$

Then,

$$vCr1(\Delta t6) = Vin + \frac{np}{nt}Vin \quad (46)$$

Seventh Stage (t_6, t_7)

The following equation describe this operational stage.

$$\Delta t7 = Lmag\frac{Imag(0)}{Vin} \quad (47)$$

Eighth Stage (t_7, t_8)

The following equation describe this operational stage.

$$\Delta t8 = Ts - \Delta t1 - \Delta t2 - \Delta t3 - \Delta t4 - \Delta t5 - \Delta t6 - \Delta t7 \quad (48)$$

Plane of phase

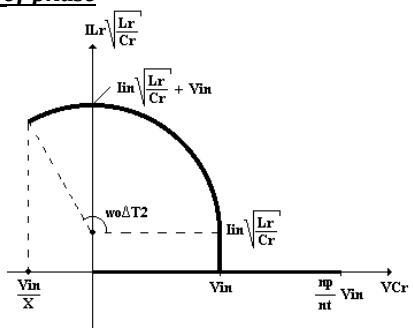

(a)

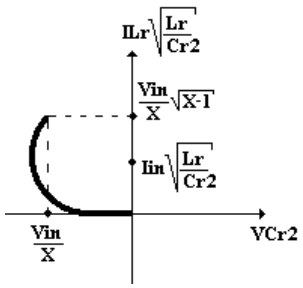

(b)

Figure 11 - Plane of phases of the FORWARD-PWM-ZVS-SR converter

Analyzing Figure 11, the non-dissipative commutation operation area for the FORWARD-PWM-ZVS-SR converter, is obtained:

$$1 \le X \le \frac{1}{4\alpha_2^2}+1 \quad (49)$$

Static Gain

The static gain can be obtained by equation (50).

$$G = \frac{Vo}{Vin} = \frac{ns}{np}\left\{D + \frac{K1}{2\pi}\left[Arccos\left(-\frac{1}{X}\right)+\frac{X+1}{X\alpha}+\frac{\alpha}{2}\right]\right\} \quad (50)$$

From equation 49 one can obtain the static gain graphic presented on Figure 12.

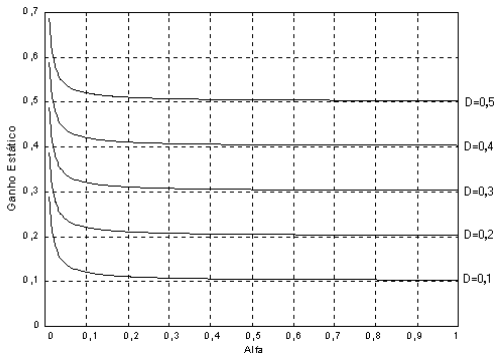

Figure 12 - Static gain for X=6.

4 – SIMULATION AND EXPERIMENTAL RESULTS

The proposed FORWARD-PWM-ZVS-SR converter (Figure 1) was studied by simulation using the P-SPICE and using the following parameter set:

S1 = IRFP460 (Mosfet);	Lf = 100μH;
S2 = Sbreak ;	Cf = 1mF;
D3 = Dbreak;	Vo = 50V;
Other diodes = MUR1560;	Io = 12A;
P_0 = 600 W;	X=6.267;
fs = 100kHz;	Lr = 2.5μH;
Cr1 = 7.5nF;	Vin = 200V.
Cr2 = 47nF;	

A prototype of the proposed FORWARD-PWM-ZVS-SR converter was built using the following parameter set:

S1 = IRFP460 (Mosfet);	Lf = 100μH;
S2 = Sbreak ;	Cf = 1mF;
D1 = 2x MUR1560;	Vo = 50V;
Other diodes = MUR1560;	Io = 12A;
P_0 = 600 W;	X=6.267;
fs = 100kHz;	Lr = 2.5μH;
Cr1 = 7.5nF;	Vin = 200V.
Cr2 = 47nF;	

Figure 13 shows the commutations in the active switches, one can see that main switch S1 do not present stresses of current and/or voltage, however, auxiliary switch S2 present

stresses of current, due to the resonance circuit, as well as the commutations are non-dissipative.

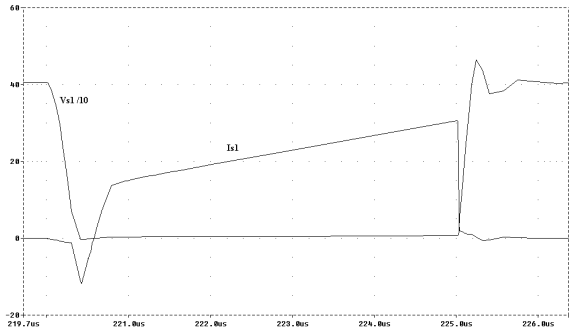

(a)

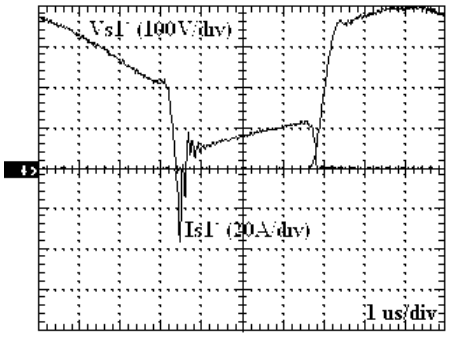

(b)

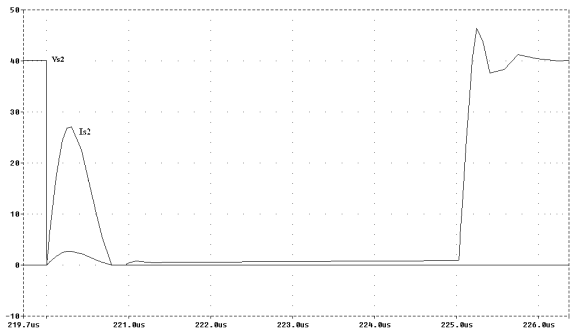

(c)

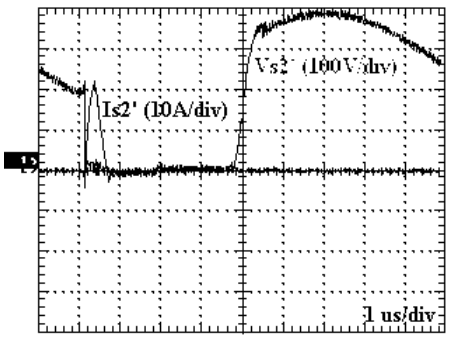

(d)

Figure 13 - Experimental Results:
a) Switch s_1 waveforms for simulated results;
b) Switch s_1 waveforms for experimental results;
c) Switch s_2 (auxiliary switch) waveforms for simulated results;
d) Switch s_2 (auxiliary switch) waveforms for experimental results.

The graph of the Figure 14 shows the curve of the efficiency of FORWARD-PWM-ZVS-SR and FORWARD-PWM, a medium efficiency of 92.8% is calculated to the FORWARD-PWM-ZVS-SR.

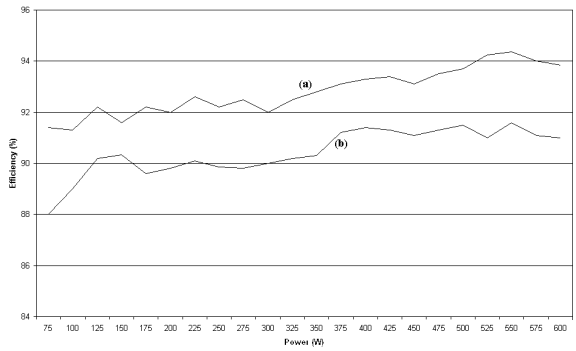

Figure 14 – Curve of efficiency:
(a) FORWARD-PWM-ZVS-SR;
(b) FORWARD-PWM.

5 - CONCLUSION

This paper presented a non-dissipative snubber associated with a Forward Converter (FORWARD-PWM-ZVS-SR). This converter works in a soft commutation way, the main switch (S1) commutates in a ZVS way and the auxiliary switch (S2) commutates in a ZCS way. The simulation and experimental results confirm the non-dissipative switching of these both switches.

This converter operates as a quasi-resonant one from the point of view of commutation and as a PWM one from the point of view of control. The main switch is not submitted to over voltages and/or over currents. The auxiliary switch is submitted to the resonant current. As result switching losses are reduced and conduction losses are almost the same as those observed in its PWM counterpart.

6 - BIBLIOGRAPHY

[1] Lee, "High-Frequency Quasi-Resonant Converter Technologies", Proceedings on the IEEE, vol. 76, nº 4, April 1988.

[2] Lee, F. C., Hua, G. and Leu, C. S., "Novel Zero-Voltage-Transition PWM Converters", IEEE PESC92, Record, pp. 55-61, Toledo, Spain.

[3] Foch, H., Meynard, T. A. and Cheron, Y., "Generalization of the Resonant Switch, Concept, Structures and Performances", Sec. European Conference on Power Electronics - EPE, pp. 239-244, 1987.

[4] Barbi, I., Bolacell, J. C. and Vieira Jr., J. B., "A Forward Pulse-Width Modulated Quasi-Resonant Converter: Analysis, Design and Experimental Results", IEEE IECON89, Record, pp. 21-26, Philadelphia, Pennsylvania, USA.

[5] Barbi, I., Hey, H. L. and Vieira Jr., J. B., "A Half-Bridge Pulse-Width Modulated Zero-Current Switched Quasi-Resonant Converter", IEEE IECON89, Record, pp. 42-47, Philadelphia, Pennsylvania, USA.

[6] Barbi, I., Oliveira, M. A. and Vieira Jr., J. B., "A Pulse-Width Modulated Zero-Voltage-Zero-Current Switched Half-Bridge Quasi-Resonant Converter", IEEE IECON89, Record, pp. 54-59, Philadelphia, Pennsylvania, USA.

[7] Vieira Jr. J. B., "Quasi-Resonant Converters: New topologies, project and analysis", PhD Thesis, UFSC, Florianópolis, SC, Brazil, 1991.

[8] de Freitas, V. J. Farias, P. S. Caparelli, J. B. Vieira Jr., H. L. Hey, D. F. Cruz, "An Optimum ZVS-PWM DC - to - DC Converter Family: Analysis, Simulation and Experimental Results". IEEE PESC92, Record, pp. 229-235, Toledo, Spain, Jul. 1992.

[9] de Freitas, D. F. Cruz, V. J. Farias, "A novel ZCS-ZVS-PWM DC-DC Buck Converter for High Power and High Switching Frequency: Analysis,

Simulation and Experimental Results". IEEE APEC93, Record, pp 693.699, San Diego, California, USA, Mar. 1993.

[10] de Freitas and P. R. C. Gomes. "A High-Power High Frequency ZCS-ZVS-PWM Buck L Converter Using a Feedback Resonant Circuit." PESC93 (IEEE publication 93CH3293-8) Record pp. 330-336 and IEEE Transation on Power Electronics -Jan/95.

[11] de Freitas, and V. J. Farias, and Nicolau P. F., "A Novel Family of DC-DC PWM Converters Using the Self Resonant Principle." PESC94 - Record - pp. 1385-1391.

[12] Barreto Luiz H. S. C., Pereira Adriano A., Farias Valdeir J., de Freitas Luiz C. and Vieira Jr João B.. ;"A Boost Converter Associated With A New Non-Dissipative Snub

ber", IEEE APEC'98, Record pp. 1077 – 1083 , Los Angeles, California, USA, Feb/1998.

[13] Barreto L. H. S. C., "Analysis, Project and Prototype of a Switching Power Supply, With High Power Factor, Using A New Snubber Non Dissipativo", MSc Thesis, UFU, Uberlândia, MG, Brazil, 1999.

[14] - Barreto L. H. S. C., Pereira A. A., Farias V. J., Freitas L. C. de and Vieira Jr J. B.;"A Boost Converter Associated With A New Non-Dissipative Snubber", CBA'98, Record pp. 1155 – 1160 , Uberlândia, Minas Gerais, Brazil, Set/1998